MCT1-mediated transport of a toxic molecule is an effective strategy for targeting glycolytic tumors

Kivanc Birsoy[1,2], **Tim Wang**[1,2,3], **Richard Possemato**[1,2], **Omer H. Yilmaz**[1,2], **Catherine E. Koch**[1,2], **Walter W. Chen**[1,2], **Amanda W. Hutchins**[1,2], **Yetis Gultekin**[1,2], **Tim R. Peterson**[1,2], **Jan E. Carette**[1,6], **Thijn R. Brummelkamp**[1,7], **Clary B. Clish**[3], and **David M. Sabatini**[1,2,3,4,5]

[1]Whitehead Institute for Biomedical Research, Nine Cambridge Center, Cambridge, MA 02142, USA

[2]Department of Biology, Massachusetts Institute of Technology (MIT), Cambridge, MA 02139, USA

[3]Broad Institute, Seven Cambridge Center, Cambridge, MA 02142, USA

[4]David H. Koch Institute for Integrative Cancer Research at MIT, 77 Massachusetts Avenue, Cambridge, MA 02139, USA

[5]Howard Hughes Medical Institute, MIT, Cambridge, MA 02139, USA

SUMMARY

There is increasing evidence that oncogenic transformation modifies the metabolic program of cells. A common alteration is the upregulation of glycolysis, and efforts to target glycolytic enzymes for anti-cancer therapy are underway. Here, we performed a genome-wide haploid genetic screen to identify resistance mechanisms to 3-bromopyruvate (3-BrPA), a drug candidate that inhibits glycolysis in a poorly understood fashion. We identified the *SLC16A1* gene product, MCT1, as the main determinant of 3-BrPA sensitivity. MCT1 is necessary and sufficient for 3-BrPA uptake by cancer cells. Additionally, MCT1 mRNA levels are the best predictor of 3-BrPA sensitivity and are most elevated in glycolytic cancer cells. Lastly, forced MCT1 expression in 3-BrPA resistant cancer cells sensitizes tumor xenografts to 3-BrPA treatment *in vivo*. Our results identify a potential biomarker for 3-BrPA sensitivity and provide proof of concept that the selectivity of cancer-expressed transporters can be exploited for delivering toxic molecules to tumors.

To whom correspondence should be addressed. sabatini@wi.mit.edu.
[6]Current address: Department of Microbiology and Immunology, Stanford University School of Medicine, Stanford, CA 94305, USA.
[7]Current address: Department of Biochemistry, Netherlands Cancer Institute, Plesmanlaan 121 1066 CX, Amsterdam, The Netherlands.

As a result of the rewiring of small molecule metabolism that accompanies oncogenic transformation, cancer cells acquire metabolic liabilities not shared by their normal counterparts[1–4]. There is great interest in identifying these liabilities and exploiting them for the development of new cancer-selective therapies[5]. Many cancer cells activate aerobic glycolysis and so exhibit high rates of glucose uptake and lactate excretion even when oxygen is available for oxidative phosphorylation[6]. Several glycolytic enzymes as well as the transporters that import glucose and export lactate are considered targets for drug development[7–13]. We undertook a loss of function genetic screen to identify genes that affect the sensitivity of cancer cells to 3-bromopyruvate (3-BrPA), a drug candidate under clinical development[14,15]. 3-BrPA has cytotoxic effects and decreases cellular energy levels by inhibiting glycolysis in a poorly understood fashion[16]. In addition to glycolytic enzymes[17–19], 3-BrPA can also inhibit several non-glycolytic enzymes[20–24] and, given its simple structure, is likely to have more than one direct protein target within cells. Thus, 3-BrPA is likely best characterized as a toxic molecule rather than a specific inhibitor of glycolysis. Here, we identify the *SLC16A1* gene product, monocarboxylate transporter 1 (MCT1), as the main determinant of 3-BrPa uptake and sensitivity, leading us to propose the therapeutic strategy of using MCT1-mediated transport to deliver toxic molecules to glycolytic tumors.

Gene-trap insertional mutagenesis in haploid or near haploid mammalian cells has enabled genome-wide loss of function screens for genes underlying basic cellular physiology [25–27]. For example, screens in the near-haploid KBM7 human cell line identified the host factors necessary for the cytotoxic effects of several viruses and microbial toxins[28–30]. To apply this approach to the study of 3-BrPA, we used retroviral infection to create a library of mutagenized haploid KBM7 cells containing ~70 million insertions, which covered approximately 98% of all genes expressed in KBM7 cells[30]. The mutagenized cells were treated with 3-BrPA and the surviving cells were expanded as a pool. Using massively parallel sequencing, insertions in the resistant population were mapped to the human genome. A proximity index analysis was used to identify genomic regions that contained multiple gene-trap insertions in close proximity. *SLC16A1* and *BSG* (Basigin) were the two most frequently inactivated genes (Fig. 1a) and had the highest degree of insertional enrichment compared to the unselected control cells (p=4.7E-121 and p=5E-29, respectively) (Supplementary Fig. 1). The highest scoring gene, *SLC16A1*, encodes MCT1, an H+ linked monocarboxylate transporter that excretes lactate from cells and is highly upregulated in a subset of cancers [31–36]. The second highest scoring gene, Basigin, is a chaperone necessary for escorting MCT1 to the plasma membrane[37,38]. To enable the in depth study of the effects of MCT1 loss, we isolated two clones (Clone A and B) that carry insertions in the first intron of the *SLC16A1* gene (Fig. 1b) and in which MCT1 protein is undetectable by immunoblotting (Fig. 1c). Consistent with the screening results, the MCT1-null cells were completely resistant to doses of 3-BrPA (Fig. 1d) that in parental KBM7 cells induce cell death accompanied by caspase-3 activation (Supplementary Fig. 1). Importantly, re-expression of MCT1 in the MCT1-null cells nearly completely restored their sensitivity to 3-BrPA (Fig. 1e). Thus, these data strongly point to MCT1 as an important determinant of 3-BrPA sensitivity in KBM7 cells.

To begin to understand how loss of MCT1 confers 3-BrPA resistance, we examined the effects of 3-BrPA on the metabolism of parental and MCT1-null KBM7 cells. In the absence of 3-BrPA, there were no differences in lactate production or oxygen consumption between the cell types (Supplementary Fig. 2), suggesting that MCT1 loss does not alter basal energy metabolism to any great extent. In contrast, 3-BrPA caused a substantial decrease in the extracellular acidification rate (ECAR), a proxy for lactate production, and total ATP levels (Fig. 2a–b) of parental, but not MCT1-null, KBM7 cells. Consistent with these findings, 3-BrPA did not affect AMPK and ACC phosphorylation, markers of energy stress[39], in MCT1-null cells while robustly increasing them in the wild type counterparts (Fig. 2b). To more completely characterize the metabolic state of cells in response to 3-BrPA, we metabolically profiled wild type and MCT1-null KBM7 cells treated with 3-BrPA. Relative to MCT1-null cells, in wild type KBM7 cells 3-BrPA caused an accumulation of the glycolytic intermediates that precede glyceraldehyde 3-phosphate, a substrate for glyceraldehyde phosphate dehydrogenase (GAPDH), but a depletion of those that come after. Furthermore, 3-BrPA treated wild type KBM7 cells accumulated intermediates of the pentose phosphate pathway, which branches off above the GADPH step of glycolysis (Fig. 2c). Additionally, the partial suppression by RNAi of GAPDH expression slows down cancer cell proliferation and sensitizes cells to 3-BrPA treatment (Supplementary Fig. 3). 3-BrPA has previously been shown to inhibit GAPDH [17] along with several other glycolytic enzymes, including hexokinase (HK2) [40,41], lactate dehydrogenase (LDH) [19], succinate dehydrogenase (SDH) [18,42], aldolase (ALDOA) [43], and pyruvate kinase (PKM) [44,45]. However, our metabolite profiling strongly implicates GAPDH inhibition as the primary cause of its anti-glycolytic effects (Fig. 2c). Altogether, these data show that MCT1-null KBM7 cells are remarkably resistant to the metabolic effects of 3-BrPA, suggesting that 3-BrPA might not enter cells in the absence of MCT1 and implicating MCT1 as a 3-BrPA transporter.

Indeed, compared to parental KBM7 cells, MCT1-null cells did not take up ^{14}C-labeled 3-BrPA (Fig. 2d). Unlabeled 3-BrPA and, to a lesser extent, known MCT1 substrates such as lactate and pyruvate, effectively competed with the uptake of radiolabeled 3-BrPA, demonstrating that the transport is specific (Supplementary Fig. 3). Moreover, consistent with the pH dependence of MCT1-mediated transport[31,46], a reduction in extracellular pH enhanced 3-BrPA uptake (Supplementary Fig. 3). Thus, MCT1 is necessary for the cellular uptake of 3-BrPA and, given its capacity to transport monocarboxylates[46], likely directly transports 3-BrPA.

Considering that there are many MCTs and SMCTs in the human genome, we took an unbiased approach to ask whether MCT1 levels are the most predictive of 3-BrPA sensitivity. In a panel of 15 cancer cell lines, we determined IC_{50} values for 3-BrPA-induced cell death and correlated them with transcriptome-wide mRNA expression data from the Cancer Cell Line Encyclopedia (CCLE) [47]. Strikingly, of the 20,000 mRNAs examined, *SLC16A1* mRNA levels were the single best predictor of 3-BrPA sensitivity (r=−0.89, p=1.4E-5) (Fig. 3a). Additionally, the expression of no other member of MCT and SMCT monocarboxylate transporter families significantly correlates with the 3-BrPA sensitivity of cancer cell lines (Fig. 3a, Supplementary Fig. 4). Finally, another monocarboxylate

transporter, Jen1p, was recently implicated as the primary carrier of 3-BrPA in yeast[48]. However, this transporter bears no homology to any human gene product.

We next asked whether MCT1 expression can also predict 3-BrPA sensitivity within a single cancer type and focused on breast cancer lines because they exhibit a particularly wide range of MCT1 expression levels (Supplementary Fig. 5). Indeed, breast cancer lines with high MCT1 protein levels are sensitive to 3-BrPA, whereas those with low to no MCT1 are resistant to even high concentrations of 3-BrPA (Fig. 3b). Stable expression of MCT1 in two breast cancer lines with low MCT1 expression (MDA-MB-231 and SK-BR-3) was sufficient to sensitize them to 3-BrPA (Fig. 3c). Additionally, as in KBM7 cells, MCT1 expression did not alter lactate production or oxygen consumption, but it did enhance ^{14}C-3-BrPA uptake (Fig. 3d). Lastly, the partial suppression by RNAi of MCT1 expression was sufficient to confer resistance to 3-BrPA to cell lines with high levels of MCT1 (BT-20, BT-549) (Fig. 3e).

To test if MCT1 expression can affect the sensitivity of established tumors to 3-BrPA, parental MDA-MB-231 cells, which express low levels of MCT1 (Supplementary Fig. 5), were injected subcutaneously into the left flanks of Nude mice, while MDA-MB-231 cells stably expressing MCT1 were injected into the contralateral flanks of the same animals. We allowed palpable subcutaneous tumors to form for 2 weeks before beginning 3-BrPA administration. After 3 weeks of 3-BrPA treatment, tumors with forced MCT1 expression were significantly smaller than those that were untreated or treated with 3-BrPA but expressing a control protein (GFP) (Fig. 3f, Supplementary Fig. 5). These results indicate that MCT1 expression is sufficient to sensitize pre-formed tumors to 3-BrPA treatment and has predictive value for determining 3-BrPA sensitivity *in vivo*.

We additionally examined if cancer cells with high levels of MCT1 expression share any metabolic properties. Using the oxygen consumption rate (OCR) to ECAR ratio as a measure of the relative contributions of OXPHOS and glycolysis to cellular energy production, we compared OCR/ECAR ratios from 15 cancer cell lines with genome-wide expression data obtained from the CCLE. Interestingly, along with two glycolytic enzymes (LDHB and PGM1), MCT1 was amongst the genes whose expression most strongly and significantly correlated with lower OCR/ECAR ratios (Fig. 4, Supplementary Fig. 5). This finding indicates that tumors which exhibit the highest rates of glycolysis are more likely to have elevated levels of MCT1 and therefore will be more sensitive to 3-BrPA treatment (Fig. 4).

Our results predict that MCT1 expression levels will serve as a biomarker for identifying tumors likely to respond to 3-BrPA treatment[14,15]. Furthermore, as we find that MCT1 expression correlates with elevated glycolysis, it may be possible to enhance the efficacy of 3-BrPA by concomitant treatment with glycolytic inhibitors so as to exploit the high glycolytic demand of tumors and the cancer-enriched expression of MCT1. It is interesting to note that small molecule inhibitors of MCT1 that inhibit lactate export from cancer cells are in development and show promise as anti-cancer therapies[11,49]. While this approach requires that MCT1 be expressed and essential for cancer cell survival[11,49], 3-BrPA treatment is distinct in that it requires only MCT1 expression to be efficacious. For example,

KBM7 cells are sensitive to 3-BrPA, but complete loss of MCT1 does not affect their viability.

Lastly, our data further suggest that the toxic effect of 3-BrPA is not a result of its anti-glycolytic effect but rather its highly alkylating nature. The stringent correlation between 3-BrPA sensitivity and expression of its transporter, but none of the previously identified metabolic targets or transporters[48,50], suggests that 3-BrPA is likely non-specifically toxic once it enters the cell. Consistent with this, 3-BrPA has non-glycolytic targets, such as V-ATPases [20], SERCAs [24], Carbonic Anhydrases [51] and HDACs [52]. Like MCT1, other transporters are also upregulated in subsets of cancers[53,54], and so it may be possible to develop toxic molecules that, in a fashion analogous to 3-BrPA, exploit these transporters to selectively enter and target cancer cells.

METHODS

Materials

Material were obtained from the following sources: antibody to MCT1 from Millipore, antibody to GAPDH from Sigma, antibodies to RPS6, ACC, AMPK, phospho-ACC, phospho-AMPK and Raptor from Cell Signaling Technologies, HRP-conjugated anti-rabbit antibody from Santa Cruz Biotechnology, lactate dehydrogenase from Roche, lactic acid and 3-BrPA from Acros Organics, RPMI-1640 media, glycine buffer solution, pyruvate, l-lactate, d-lactate puromycin, and polybrene from Sigma, blasticidin from Invivogen, [14]C-3BrPA from Moravek Biosciences, Matrigel and Cell-Tak from BD Biosciences, IMDM from US Biologicals. Cell lines were obtained from ATCC. Lentiviral shRNAs were obtained from the The RNAi Consortium (TRC) collection of the Broad Institute. The TRC numbers for the shRNAs used are TRCN0000072186 (GFP), TRCN0000038339 (MCT1_1), TRCN0000038340 (MCT1_2), TRCP0000982283 (GAPDH_1) and TRCP0000982283 (GAPDH_2). Primer sequences for cloning MCT1 into pMXs-IRES-blasticidin and PLJM1-puro are indicated in the Supplementary Table 1.

Cell Culture and Virus transduction

KBM7 cells were cultured in IMDM supplemented with with 10% IFS and penicillin/ streptomycin. All other cell lines in this study were cultured in RPMI supplemented with 10% FBS. KBM7, MDA-MB-231 and Sk-Br-3 cell lines stably overexpressing human MCT1 or GFP were generated by infection with lentiviruses expressing the corresponding cDNAs and selected for blasticidin (10 μg/ml) or puromycin resistance (4 μg/ml) for 3 days, respectively. Similarly BT-20, KBM7, MDA-MB-468 and BT-549 expressing shRNAs for MCT1 and GAPDH were generated by infection with lentiviruses expressing the corresponding shRNAs (Supplementary Table 1) and spin-infected via a 30-min spin at 2,250 rpm in media containing 4 μg/ml polybrene. Cells were next selected with puromycin.

Haploid Cell Screening

A haploid cell genetic screen with 3-BrPA was performed using 100 million mutagenized KBM7 cells as described previously [30]. Mutagenized haploid KBM-7 cells were exposed to 50 μM 3-BrPA for 3 weeks. Surviving clones were harvested and genomic DNA was

isolated and insertions were amplified. The sequences flanking retroviral insertion sites were mapped to the human genome using inverse PCR followed by Illumina sequencing. Genomic regions with a high density of insertions were identified using the proximity index for a given insertion. Additionally, the statistical enrichment of insertions at a given locus in the selected population was calculated by comparing the number of inactivating insertions to those in the untreated control dataset via a Fisher's Exact Test. Individual clones were isolated and genomic DNA for individually selected clones were isolated using a genomic DNA isolation kit (Qiagen). Genomic insertions were identified by inverse PCR and subsequent sequencing as described previously [25].

Metabolic assays

The bioenergetic profiles of KBM7 and MDA-MB-231 cells in response to 3-BrPA were determined using a Seahorse Bioscience XF24 Extracellular Flux Analyzer (Seahorse Bioscience). For the indicated experiments, 250,000 KBM7 or 40,000 MDA-MB-231 cells seeded in Seahorse tissue culture plates using unbuffered RPMI (10 mM Glucose). KBM7 cells were attached to the plates using CellTak (Clontech) one hour prior to the start of the experiment. For AUC (area under the curve) OCR and ECAR measurements, three consecutive readings were performed for each cell line. For experiments where 3-BrPA is used, after 3 consecutive readings, 50 μM 3-BrPA was injected through port A and ECAR and OCAR levels were measured. Lactate production was measured as described previously[55]. For ATP assays, 20,000 cells were seeded and treated for 60 min with indicated amounts of 3-BrPA and relative ATP levels compared to untreated cells were determined using a luciferase-based assay (Promega). For metabolite measurements, 10 million wild type and MCT1 null KBM7 cells were cultured for 1 hour in presence of 50 μM 3-BrPA before metabolite extraction. Then, cells were rapidly washed three times with cold PBS, and then metabolites were extracted by addition of 80% ice-cold methanol followed after incubation on dry ice for 15 min. Endogenous metabolite profiles were obtained using LC-MS as described[56]. Metabolite levels (n=3) were normalized to cell number.

3-BrPA uptake assay

Wild type KBM7 or MCT1-null cells were seeded in HBSS and exposed for up to 20 minutes to 100 μM C^{14}-labeled 3-BrPA (6.8 mCi/mmole) (Moravek) with or without competitor molecules like 3-BrPA, pyruvate, L-lactate and D-lactate. Cells were washed with cold HBSS, lysed in a NaOH buffer, and uptake measured using a liquid scintillation counter.

Cell Survival Assays

Cells (5,000–20,000 cells) were seeded in 96-well plates and treated with indicated amounts of 3-BrPA. After 3 days of treatment, CellTiter-Glo (Promega) and/or CyQuant (Invitrogen) were used to measure cell cycle arrest or cell death percentage for each concentration compared to untreated cells. FACS analysis with Annexin V and 7AAD staining was performed according to manufacturer's manual (BD Pharmingen).

Correlation Analysis

15 cell lines (BT-474, BT-549, CAKI-1, CAL-51, HCC-70, Hs 578T, Jurkat, MDA-MB-157, MDA-MB-231, MDA-MB-453, MDA-MB-468, PC-3, SK-BR-3, T47D, ZR-75–1) were treated with 3-BrPA (0–300 μM). After 3 days, cell viability was quantified via CellTiter-Glo assay and an IC_{50} from the resulting dose-response curve was interpolated using a nonlinear regression model. Transcriptome-wide normalized mRNA levels from gene expression profiling experiments performed on the Affymetrix Human Genome U133 Plus 2.0 chip were obtained from the CCLE for all 15 cell lines. The mRNA expression pattern across all 15 samples for each of the genes was then correlated with the IC_{50} values. A similar correlation analysis was performed using OCR/ECAR values for each cell line.

Immunoblotting and Immunohistochemistry

Briefly, cells were rinsed twice in ice-cold PBS and harvested in a standard lysis buffer containing 50mM Hepes, pH 7.4, 40mM NaCl, 2mM EDTA, 1.5mM orthovanadate, 50mM NaF, 10mM pyrophosphate, 10mM glycerophosphate, protease inhibitors (Roche) and 1% Triton-X-100. Proteins from total lysates were resolved by 8–12% SDS-PAGE, and analyzed by immunoblotting using indicated antibodies (1:1000)[55]. For quantitation, ImageJ software was used and the signals were normalized using an equal loading control (RPS6/Raptor). Immunohistochemistry was performed on formalin-fixed paraffin embedded sections using a boiling Dako antigen retrieval method (Dako). A 1:500 dilution of the anti-MCT1 antibody was used for staining.

Mouse studies

All animal studies and procedures were approved by the MIT Institutional Animal Care and Use Committee. 6–10 week old nude mice (Taconic) were used for generating all xenografts. In subcutaneous xenografts, mice were injected at two sites in the dorsal region, under isofluorane anesthesia with 100 μl/injection of tumor cell suspension in RPMI with 20% matrigel. 2.5 million MDA-MB-231 cells were injected. After 2 weeks, tumors were measured and mice were separated for PBS and 3-BrPA treatment (8 mg/kg). After 3 weeks, tumors were harvested, their dimensions were measured with a caliper and tumor volume estimated according to the formula: (0.5*W*L*L). Tumors were fixed in formalin for later processing.

Supplementary Material

Refer to Web version on PubMed Central for supplementary material.

Acknowledgments

References

1. Vander Heiden MG. Targeting cancer metabolism: a therapeutic window opens. Nat Rev Drug Discov. 2011; 10:671–684. [PubMed: 21878982]

2. Thompson CB. Rethinking the Regulation of Cellular Metabolism. Cold Spring Harb Symp Quant Biol. 2012

3. DeBerardinis RJ, Thompson CB. Cellular metabolism and disease: what do metabolic outliers teach us? Cell. 2012; 148:1132–1144. [PubMed: 22424225]

4. Tennant DA, Duran RV, Gottlieb E. Targeting metabolic transformation for cancer therapy. Nat Rev Cancer. 2010; 10:267–277. [PubMed: 20300106]

5. Birsoy K, Sabatini DM, Possemato R. Untuning the tumor metabolic machine: Targeting cancer metabolism: a bedside lesson. Nat Med. 2012; 18:1022–1023. [PubMed: 22772555]

6. Warburg O. On respiratory impairment in cancer cells. Science. 1956; 124:269–270. [PubMed: 13351639]

7. Pelicano H, Martin DS, Xu RH, Huang P. Glycolysis inhibition for anticancer treatment. Oncogene. 2006; 25:4633–4646. [PubMed: 16892078]

8. Xu RH, et al. Inhibition of glycolysis in cancer cells: a novel strategy to overcome drug resistance associated with mitochondrial respiratory defect and hypoxia. Cancer Res. 2005; 65:613–621. [PubMed: 15695406]

9. Sonveaux P, et al. Targeting lactate-fueled respiration selectively kills hypoxic tumor cells in mice. J Clin Invest. 2008; 118:3930–3942. [PubMed: 19033663]

10. Vander Heiden MG, et al. Identification of small molecule inhibitors of pyruvate kinase M2. Biochem Pharmacol. 2010; 79:1118–1124. [PubMed: 20005212]

11. Le Floch R, et al. CD147 subunit of lactate/H+ symporters MCT1 and hypoxia-inducible MCT4 is critical for energetics and growth of glycolytic tumors. Proc Natl Acad Sci U S A. 2011; 108:16663–16668. [PubMed: 21930917]

12. Wood TE, et al. A novel inhibitor of glucose uptake sensitizes cells to FAS-induced cell death. Mol Cancer Ther. 2008; 7:3546–3555. [PubMed: 19001437]

13. Stein M, et al. Targeting tumor metabolism with 2-deoxyglucose in patients with castrate-resistant prostate cancer and advanced malignancies. Prostate. 2010; 70:1388–1394. [PubMed: 20687211]

14. Pedersen PL. 3-bromopyruvate (3BP) a fast acting, promising, powerful, specific, and effective "small molecule" anti-cancer agent taken from labside to bedside: introduction to a special issue. J Bioenerg Biomembr. 2012; 44:1–6. [PubMed: 22382780]

15. Ko YH, et al. A translational study "case report" on the small molecule "energy blocker" 3-bromopyruvate (3BP) as a potent anticancer agent: from bench side to bedside. J Bioenerg Biomembr. 2012; 44:163–170. [PubMed: 22328020]

16. Shoshan MC. 3-bromopyruvate: Targets and outcomes. J Bioenerg Biomembr. 2012

17. Ganapathy-Kanniappan S, et al. Glyceraldehyde-3-phosphate dehydrogenase (GAPDH) is pyruvylated during 3-bromopyruvate mediated cancer cell death. Anticancer Res. 2009; 29:4909–4918. [PubMed: 20044597]

18. Pereira da Silva AP, et al. Inhibition of energy-producing pathways of HepG2 cells by 3-bromopyruvate. Biochem J. 2009; 417:717–726. [PubMed: 18945211]

19. Dell'Antone P. Targets of 3-bromopyruvate, a new, energy depleting, anticancer agent. Med Chem. 2009; 5:491–496. [PubMed: 19534685]

20. Dell'Antone P. Inactivation of H+-vacuolar ATPase by the energy blocker 3-bromopyruvate, a new antitumour agent. Life Sci. 2006; 79:2049–2055. [PubMed: 16908033]

21. Blessinger KJ, Tunnicliff G. Kinetics of inactivation of 4-aminobutyrate aminotransferase by 3-bromopyruvate. Biochem Cell Biol. 1992; 70:716–719. [PubMed: 1476707]

22. Tunnicliff G, Ngo TT. Mechanism of inactivation of brain glutamic decarboxylase by 3-bromopyruvate. Int J Biochem. 1978; 9:249–252. [PubMed: 648707]

23. Arendt T, Schugens MM, Marchbanks RM. Reversible inhibition of acetylcholine synthesis and behavioural effects caused by 3-bromopyruvate. J Neurochem. 1990; 55:1474–1479. [PubMed: 2213005]

24. Jardim-Messeder D, Camacho-Pereira J, Galina A. 3-Bromopyruvate inhibits calcium uptake by sarcoplasmic reticulum vesicles but not SERCA ATP hydrolysis activity. Int J Biochem Cell Biol. 2012; 44:801–807. [PubMed: 22343412]

25. Carette JE, et al. Haploid genetic screens in human cells identify host factors used by pathogens. Science. 2009; 326:1231–1235. [PubMed: 19965467]

26. Layton JE. Undertaking a successful gynogenetic haploid screen in zebrafish. Methods Mol Biol. 2009; 546:31–44. [PubMed: 19378096]

27. Elling U, et al. Forward and reverse genetics through derivation of haploid mouse embryonic stem cells. Cell Stem Cell. 2011; 9:563–574. [PubMed: 22136931]

28. Carette JE, et al. Ebola virus entry requires the cholesterol transporter Niemann-Pick C1. Nature. 2011; 477:340–343. [PubMed: 21866103]

29. Guimaraes CP, et al. Identification of host cell factors required for intoxication through use of modified cholera toxin. J Cell Biol. 2011; 195:751–764. [PubMed: 22123862]

30. Carette JE, et al. Global gene disruption in human cells to assign genes to phenotypes by deep sequencing. Nat Biotechnol. 2011; 29:542–546. [PubMed: 21623355]

31. Morris ME, Felmlee MA. Overview of the proton-coupled MCT (SLC16A) family of transporters: characterization, function and role in the transport of the drug of abuse gamma-hydroxybutyric acid. AAPS J. 2008; 10:311–321. [PubMed: 18523892]

32. Pinheiro C, et al. Monocarboxylate transporter 1 is up-regulated in basal-like breast carcinoma. Histopathology. 2010; 56:860–867. [PubMed: 20636790]

33. Pinheiro C, et al. Monocarboxylate transporters 1 and 4 are associated with CD147 in cervical carcinoma. Dis Markers. 2009; 26:97–103. [PubMed: 19597291]

34. Mathupala SP, Parajuli P, Sloan AE. Silencing of monocarboxylate transporters via small interfering ribonucleic acid inhibits glycolysis and induces cell death in malignant glioma: an in vitro study. Neurosurgery. 2004; 55:1410–1419. discussion 1419. [PubMed: 15574223]

35. Koukourakis MI, Giatromanolaki A, Bougioukas G, Sivridis E. Lung cancer: a comparative study of metabolism related protein expression in cancer cells and tumor associated stroma. Cancer Biol Ther. 2007; 6:1476–1479. [PubMed: 17881895]

36. Pinheiro C, et al. Increased expression of monocarboxylate transporters 1, 2, and 4 in colorectal carcinomas. Virchows Arch. 2008; 452:139–146. [PubMed: 18188595]

37. Poole RC, Halestrap AP. Interaction of the erythrocyte lactate transporter (monocarboxylate transporter 1) with an integral 70-kDa membrane glycoprotein of the immunoglobulin superfamily. J Biol Chem. 1997; 272:14624–14628. [PubMed: 9169423]

38. Kirk P, et al. CD147 is tightly associated with lactate transporters MCT1 and MCT4 and facilitates their cell surface expression. EMBO J. 2000; 19:3896–3904. [PubMed: 10921872]

39. Mihaylova MM, Shaw RJ. The AMPK signalling pathway coordinates cell growth, autophagy and metabolism. Nat Cell Biol. 2011; 13:1016–1023. [PubMed: 21892142]

40. Rodrigues-Ferreira C, da Silva AP, Galina A. Effect of the antitumoral alkylating agent 3-bromopyruvate on mitochondrial respiration: role of mitochondrially bound hexokinase. J Bioenerg Biomembr. 2012

41. Ko YH, et al. Advanced cancers: eradication in all cases using 3-bromopyruvate therapy to deplete ATP. Biochem Biophys Res Commun. 2004; 324:269–275. [PubMed: 15465013]

42. Sanborn BM, Felberg NT, Hollocher TC. The inactivation of succinate dehydrogenase by bromopyruvate. Biochim Biophys Acta. 1971; 227:219–231. [PubMed: 5550821]

43. Meloche HP, Luczak MA, Wurster JM. The substrate analog, bromopyruvate, as both a substrate and alkylating agent for 2-keto-3-deoxy-6-phosphogluconic aldolase. Kinetic and stereochemical studies. J Biol Chem. 1972; 247:4186–4191. [PubMed: 5035689]

44. Yun SL, Suelter CH. Modification of yeast pyruvate kinase by an active site-directed reagent, bromopyruvate. J Biol Chem. 1979; 254:1811–1815. [PubMed: 370116]

45. Acan NL, Ozer N. Modification of human erythrocyte pyruvate kinase by an active site-directed reagent: bromopyruvate. J Enzyme Inhib. 2001; 16:457–464. [PubMed: 11916152]

46. Halestrap AP. The monocarboxylate transporter family--Structure and functional characterization. IUBMB Life. 2012; 64:1–9. [PubMed: 22131303]

47. Barretina J, et al. The Cancer Cell Line Encyclopedia enables predictive modelling of anticancer drug sensitivity. Nature. 2012; 483:603–607. [PubMed: 22460905]

48. Lis P, et al. Transport and cytotoxicity of the anticancer drug 3-bromopyruvate in the yeast Saccharomyces cerevisiae. J Bioenerg Biomembr. 2012; 44:155–161. [PubMed: 22359102]

49. Murray CM, et al. Monocarboxylate transporter MCT1 is a target for immunosuppression. Nat Chem Biol. 2005; 1:371–376. [PubMed: 16370372]

50. Queiros O, et al. Butyrate activates the monocarboxylate transporter MCT4 expression in breast cancer cells and enhances the antitumor activity of 3-bromopyruvate. J Bioenerg Biomembr. 2012; 44:141–153. [PubMed: 22350013]

51. Gothe PO, Nyman PO. Inactivation of human erythrocyte carbonic anhydrases by bromopyruvate. FEBS Lett. 1972; 21:159–164. [PubMed: 11946500]

52. Thangaraju M, et al. Transport by SLC5A8 with subsequent inhibition of histone deacetylase 1 (HDAC1) and HDAC3 underlies the antitumor activity of 3-bromopyruvate. Cancer. 2009; 115:4655–4666. [PubMed: 19637353]

53. Ganapathy V, Thangaraju M, Prasad PD. Nutrient transporters in cancer: relevance to Warburg hypothesis and beyond. Pharmacol Ther. 2009; 121:29–40. [PubMed: 18992769]

54. Gupta N, et al. Upregulation of the amino acid transporter ATB0,+ (SLC6A14) in colorectal cancer and metastasis in humans. Biochim Biophys Acta. 2005; 1741:215–223. [PubMed: 15905073]

55. Possemato R, et al. Functional genomics reveal that the serine synthesis pathway is essential in breast cancer. Nature. 2011; 476:346–350. [PubMed: 21760589]

56. Finley LW, et al. Skeletal muscle transcriptional coactivator PGC-1alpha mediates mitochondrial, but not metabolic, changes during calorie restriction. Proc Natl Acad Sci U S A. 2012; 109:2931–2936. [PubMed: 22308395]
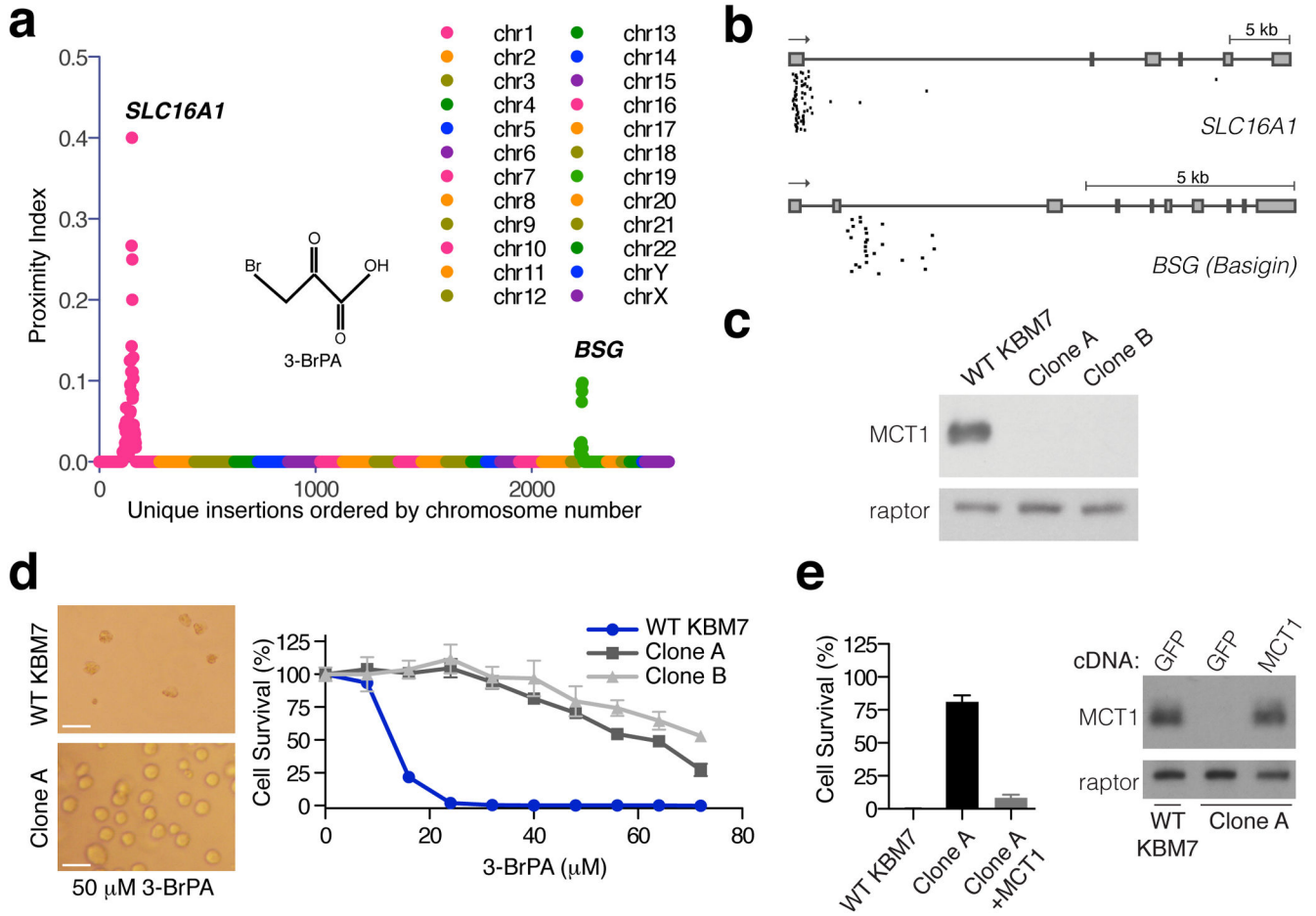
Figure 1. Haploid cell genetic screening identifies MCT1 as required for 3-BrPA sensitivity
(**a**) Mutagenized KBM7 cells were treated with 3-BrPA and resistant clones were pooled.
Gene–trap insertion sites were identified by massively parallel sequencing and mapped to
the human genome. The Y-axis represents the proximity index, a measure of the local
density of insertions. The X-axis represents the insertion sites ordered by their genomic
position. (**b**) Map of unique insertion sites in the *SLC16A1 (MCT1)* and *BSG* (Basigin) genes
in the surviving cell population. Boxes denote exons. (**c**) Immunoblotting for MCT1 protein
in two clonally derived cell lines containing gene trap insertions in *SLC16A1* (Clone A and
B). (**d**) Resistance of MCT1-null KBM7 clones to 3-BrPA (50 μM) compared to wild type
KBM7 cells. Microscopic analysis (Left) and survival curves (Right) of wild type and
MCT1-null KBM7 cells after 3 days of 3-BrPA treatment. Error bars are ± SEM. Scale bar,
20 microns. (**e**) Exogenous expression of MCT1 in MCT1-null KBM7 cells restores their
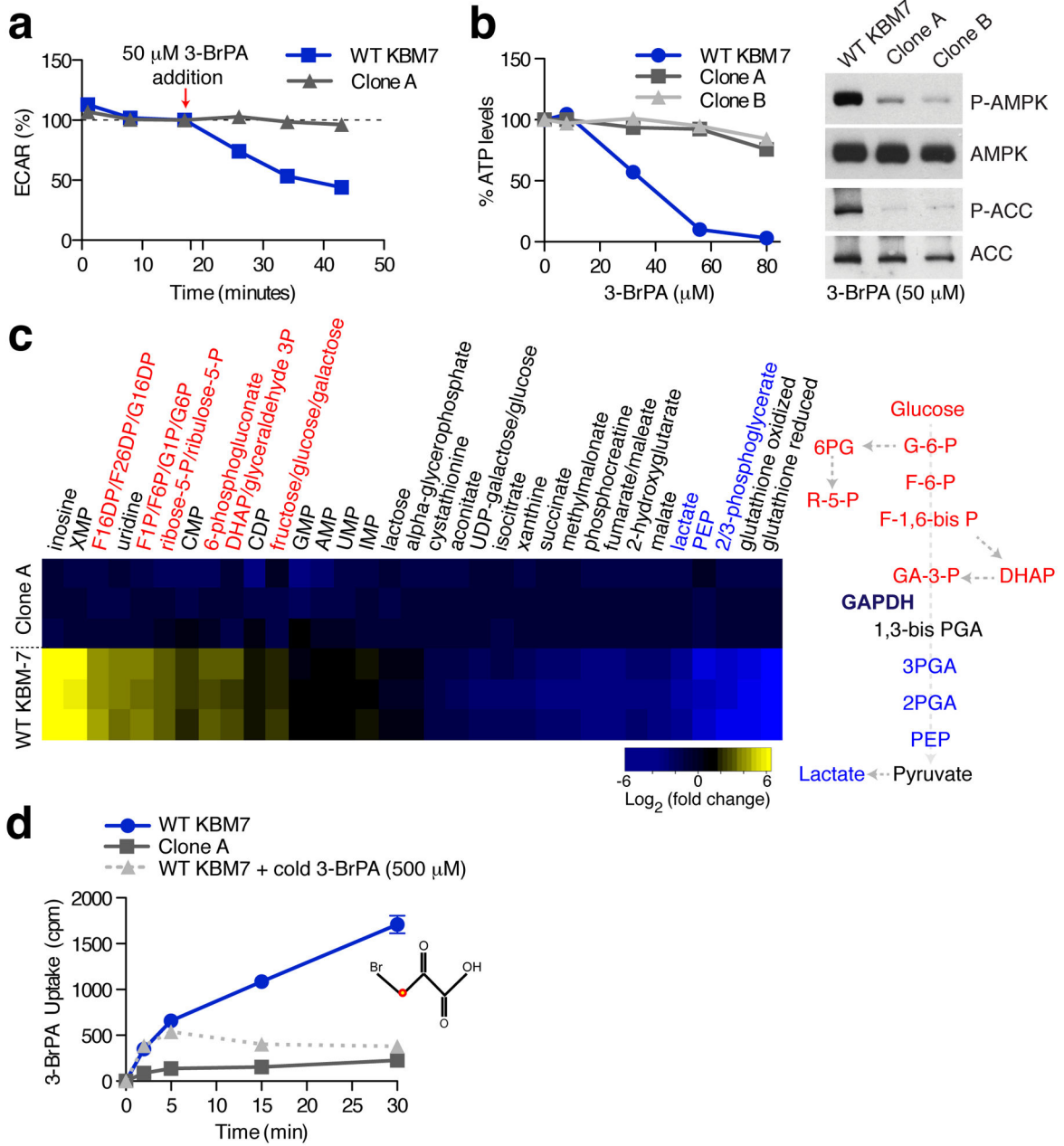sensitivity to 3-BrPA. Error bars are ± SEM (n = 3).

Figure 2. MCT1-null cells are immune to the metabolic effects of 3-BrPA and do not transport it
(**a**) Extracellular Flux Analysis of wild type and MCT1-null KBM7 cells upon 3-BrPA (50 μM) addition. Changes in ECAR, a proxy for lactate production, were monitored upon the addition of 50 μM 3-BrPA. Results are displayed as a percentage of the ECAR reading immediately before 3-BrPA addition. Error bars are ± SEM (n = 10). (**b**) Intracellular ATP levels in wild type and MCT1-null KBM7 cells were determined after treatment for 60 minutes with the indicated concentrations of 3-BrPA using a luciferase-based assay. Error bars are ± SEM (n = 6). Immunoblots show phosphorylation status of AMPK and ACC in wild type and MCT1-null KBM7 cell after treatment with 3-BrPA (50 μM). (**c**) Heat map of relative metabolite changes between wild type and MCT1-null KBM7 cells upon 3-BrPA

treatment. Yellow to blue colored bar indicates degree of change ($\log_2$) in metabolite abundance relative to MCT1-null KBM7 cells. Cells were cultured for 1 hour with 50 μM 3-BrPA and intracellular metabolites were obtained and analyzed by LC-MS (n = 3).

(**d**) ^{14}C-3-BrPA uptake in MCT1-null and wild type KBM7 cells in the presence/absence of excess unlabeled 3-BrPA (500 μM). Error bars are ± SEM (n = 3). Note that in some instances error bars are too small to see or are hidden by a symbol.
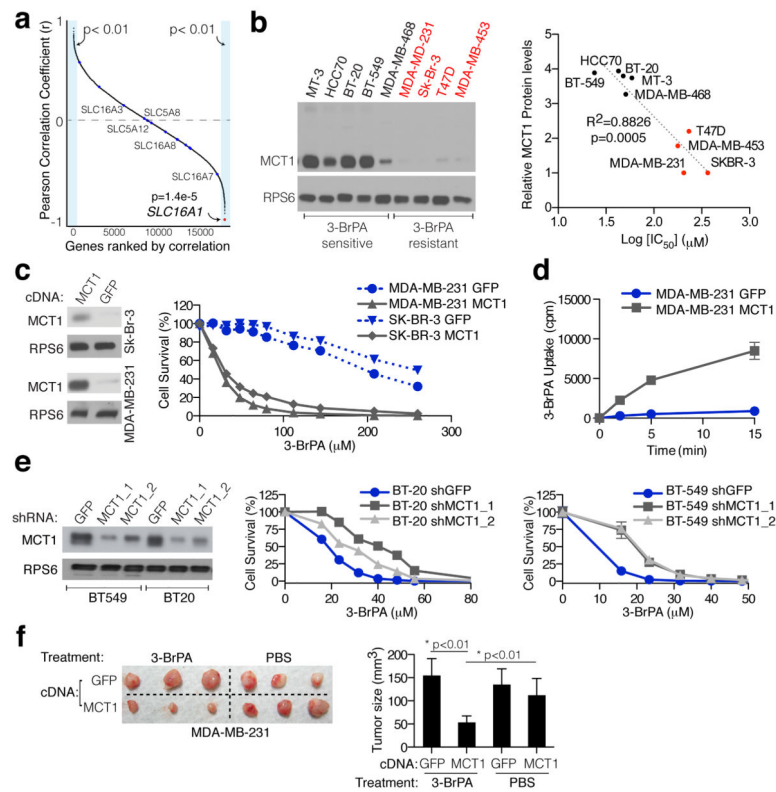
Figure 3. MCT1 expression is the predominant determinant of 3-BrPA sensitivity in cancer cells
(**a**) The concentration of 3-BrPA at which 50% cell growth inhibition occurred after 3 days of administration (IC_{50}) was determined for 15 cancer cell lines. These values were correlated with transcriptome-wide mRNA expression data from the Cancer Cell Line Encyclopedia (CCLE) and the resulting Pearson correlation coefficients were sorted and plotted. The red dot indicates *SLC16A1 (MCT1)*, whereas blue dots indicate members of MCT and SMCT family of transporters. Names of all members of these families shown to transport lactate are indicated on the plot. (**b**) Immunoblot shows MCT1 protein levels for 9 different breast cancer cell lines (Left). Relative protein levels correlated with the corresponding IC_{50} values for 3-BrPA for each cell line (Right). (**c**) Immunoblot for MCT1 levels in SK-BR-3 and MDA-MB-231 cells expressing a control GFP protein or MCT1 (Left). Survival curves of indicated cell lines expressing the MCT1 cDNA and treated with 3-BrPA (Right). Error bars are ± SEM (n = 3). (**d**) ^{14}C-3-BrPA uptake in parental and MCT1-overexpressing MDA-MB-231 cells. Error bars are ± SEM (n = 3). (**e**) Immunoblots and survival curves upon 3-BrPA treatment for indicated cell lines expressing shRNAs targeting a control GFP protein or MCT1 (MCT1_1 and MCT1_2). Error bars are ± SEM (n = 3). (**f**) Representative photographs (Left) and average weights (Right) of tumors formed by MDA-MB-231 cells expressing the MCT1 or GFP cDNA after 3 weeks of treatment with vehicle or 3-BrPA (8 mg/kg). Error bars are ± SD (n = 5). Note that in some instances error bars are too small to see or are hidden by a symbol.
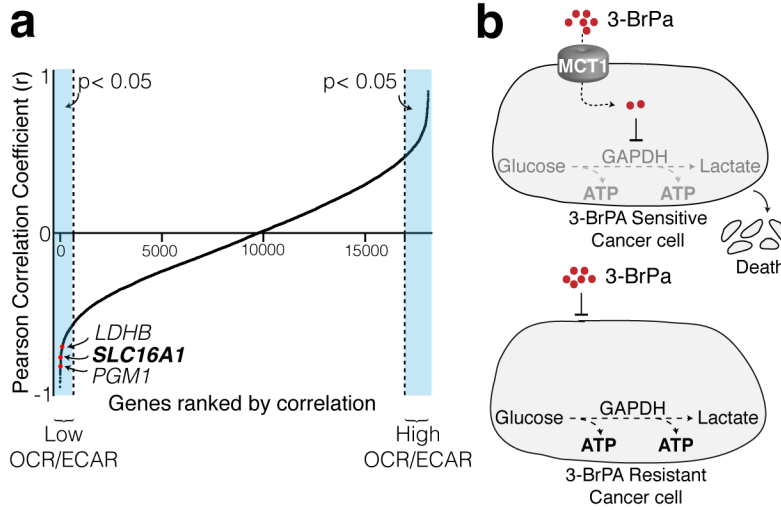
Figure 4. MCT1 expression correlates with glycolysis upregulation in cancer cells
(**a**) OCR/ECAR values were determined for 15 cell lines using the Seahorse Extracellular Flux Analyzer. These values were correlated with transcriptome-wide mRNA expression data from the Cancer Cell Line Encyclopedia (CCLE) and the resulting Pearson correlation coefficients were sorted and plotted. (**b**) Schematic illustration of the toxic cargo delivery strategy using 3-BrPA. Glycolytic cancer cells express high levels of MCT1 and are sensitive to 3-BrPA. Cancer cells with low/no levels of MCT1 are resistant to 3-BrPA.